Chemical physics of air clathrate hydrates

Werner F.Kuhs*, Alice Klapproth* and Bertrand Chazallon*†

*Mineralogisch-Kristallographisches Institut, Universität Göttingen, Goldschmidtstr.1, 37077 Göttingen, GERMANY
†LPCML, UMR 5620, Université Claude-Bernard Lyon I, 43 Boulevard du 11 novembre 1918, 69622 Villeurbanne, FRANCE

Abstract: The chemico-physical properties of air clathrate hydrates are reviewed, based both on laboratory experiments and observations made in ice core studies. Recent results on gas fractionation, cage occupancies and compressibilities obtained in laboratory experiments are presented. Finally, concepts for a description of clathrate nucleation, growth and decomposition are discussed.

1. Introduction

Air clathrate hydrates are observed in deeper parts of polar ice sheets. In the presence of ice and with the increasing pressure at larger depths air bubbles become thermodynamically unstable against air clathrate hydrates. The occurence of air hydrates in ice sheets was predicted by Miller [1] based on observations by Gow et al. [2] in bubble-free but air-rich ice cores from Byrd station in Antarctica. Detailed descriptions of the properties of gas-filled inclusions forming in originally bubble-free ice, some time after the cores were drilled, are given by Gow [3]. Evidence in support of clathrate hydrate formation from gas-filled inclusions was first presented by Gow and Williamson [4]. The first documented observations of air hydrates in ice cores were made by Shoji & Langway [5] in the Dye-3 Greenland ice core. Since then they have repeatedly been observed in ice cores from Greenland and Antarctica as transparent inclusions embedded in the ice matrix. It is the purpose of this article to review the current state of knowledge on the various properties of air clathrate hydrates.

Clathrate hydrates form a class of inclusion compounds in which gases are imprisoned in a host structure formed by H-bonded water molecules. The guest molecules interact with the host framework through van der Waals and electrostatic interactions to stabilize the structure, which is thermodynamically unstable when empty. The degree of filling is variable and depends on the nature of the gas, pressure (fugacity) and temperature. The present state-of-the-art research in clathrate hydrates is detailed by Sloan [6]. Two main crystallographic structures are known in which clathrate hydrates crystallize [7]. Air hydrates usually form a type II crystal structure [8], which is built from 8 large and 16 small cages per unit cell. Nitrogen, oxygen, but possibly also other gases contained in the air enter into these cages. Based partly on recent results

Physics of Ice Core Records
Edited by T. Hondoh
Hokkaido University Press, 2000, Sapporo

obtained in Göttingen, the review examines first the equilibrium properties of air clathrates before discussing aspects of non-equilibrium, growth and decomposition. The focus will generally be on the properties of some relevance to processes in polar ice sheets.

2. Equilibrium properties

2.1 Stability field

The decomposition lines for N_2, O_2 and air clathrate hydrates have already been given by Miller [1] based on a single experimental data point at –35 °C and the established phase diagram near the triple point (water - ice Ih - clathrate). These curves have frequently been cited in the literature [e.g. 4] but it seems they have never been independently verified. Very recently we have undertaken a series of experiments to establish the decomposition lines of N_2, O_2 and air clathrates. The decomposition pressure was measured at various temperatures in the range –20 to 0 °C. The decomposition lines were found to be at slightly lower pressures than those found by Miller (Fig. 1). It is also worthwhile to note that the computed decomposition line for N_2 clathrate (based on the thermodynamic theory of van der Waals and Platteeuw [9] and calculated with the program CSMHYD [6]) does not correctly reproduce the experimental values. The new experimental values are in agreement with observations from the Byrd ice core, where clathrates were observed [10] at shallower depths than predicted by Miller's curves [1]. For convenience, the following formula may be used to calculate the decomposition line

$$\log_{10} P = a + b/T$$

with P given in bar and T in K. The fitted constants for N_2, O_2 and air respectively are a: 4.77(5), 5.17(2) and 4.63(11); b: –710(14), –850(6), –683(28), with the estimated error given in brackets.

As a general comment, the calculation of stability fields using the statistical thermodynamic theory of van der Waals & Platteeuw [9] delivers reasonable estimates for most mixed gases in equilibrium with liquid water [6]. However, more uncertain are the predicted stability fields of pure and mixed gas hydrates with respect to ice Ih. This is not really surprising as the empirical parameters of the gas-water interaction are usually optimized using the experimental three-phase hydrate+gas+liquid(water) data of the pure systems.

2.2 Gas fractionation

There are currently several investigations concerned with possible fractionation effects of natural air hydrates. The question was already put into focus with the first Raman-scattering study on natural air-hydrates from the DYE-3 ice core in which Nakahara et al. [12] found a substantial oxygen enrichment with a N_2/O_2 ratio of 1.7. Later Pauer et al. [13, 14], working on samples from the GRIP-core well below the transition zone (i.e. below the coexistence range of air hydrates and air bubbles), found N_2/O_2 ratios slightly below but close to the atmospheric value of 3.73. In contrast to these findings samples from the transition zone of Antarctic ice cores exhibit a clear fractionation effect as measured by micro-Raman spectroscopy, both in the clathrates and in the air bubbles [15]. It should also be noted that the N_2/O_2 ratio varies as a function of crystal

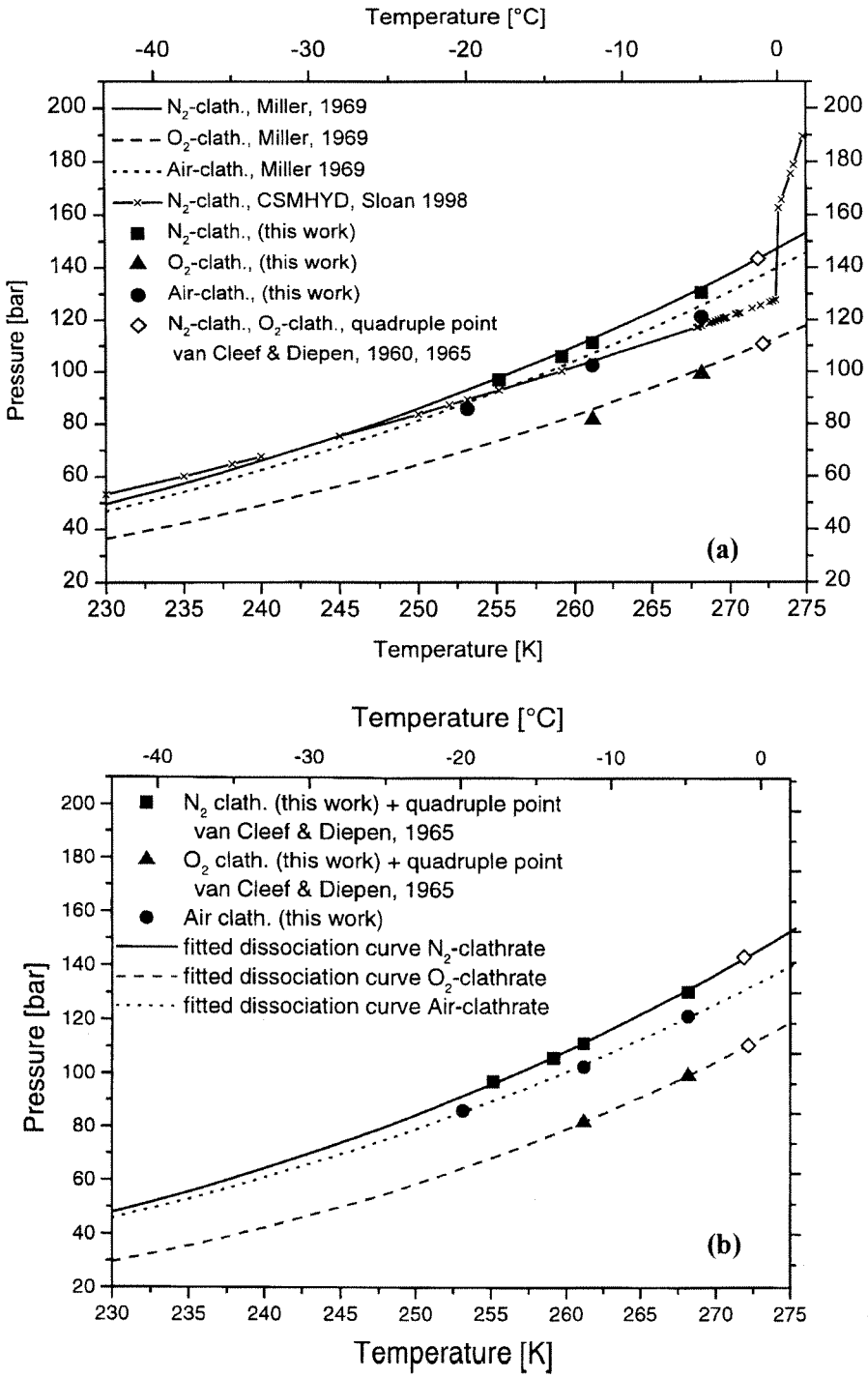

Figure 1: The decomposition curves for N_2, O_2 and air clathrate hydrates. (a) The experimental curves as established by Miller [1] and the calculated curve obtained from CSMHYD [6], which is in clear disagreement with experimental data presented in this work. (b) Experimental data obtained in this work and fitted decomposition curves (see text). The fit was made including the experimental quadruple points measured by van Cleef and Diepen [11].

orientation in a (polarised) Raman spectrum [16]. According to the theory of van der Waals and Plaatteuw [9], a reaction of air and water or ice to air hydrate should produce at least initially O_2-enriched crystals. With a limited reservoir of air, as in air bubbles included in ice, one has to expect the subsequent formation of a zoned crystal with a steadily increasing content of N_2. However, this stage of clathrate formation can very rarely be observed in ice cores. Rather, the final product is likely to regrow (see section 4.2 below) and, consequently, will exhibit a rather homogeneous distribution of oxygen and nitrogen within one crystallite [14]. If there is no mechanical separation of a growing clathrate from the remaining air bubble, nor any preferential out-diffusion of air constituents, the final composition after the regrowth will be identical to the initial composition of the untransformed air bubble. The fractionation effect has been established quantitatively by physico-chemical work in our laboratory where air-hydrates were formed from normal air with a N_2/O_2 ratio of 3.73 [17]. The N_2/O_2 ratio in the solid clathrate was measured by Raman spectroscopy. In contrast to the situation for air bubbles in ice cores, the reservoir of air was considered to be infinite (due to the large volume of the compressor system) and

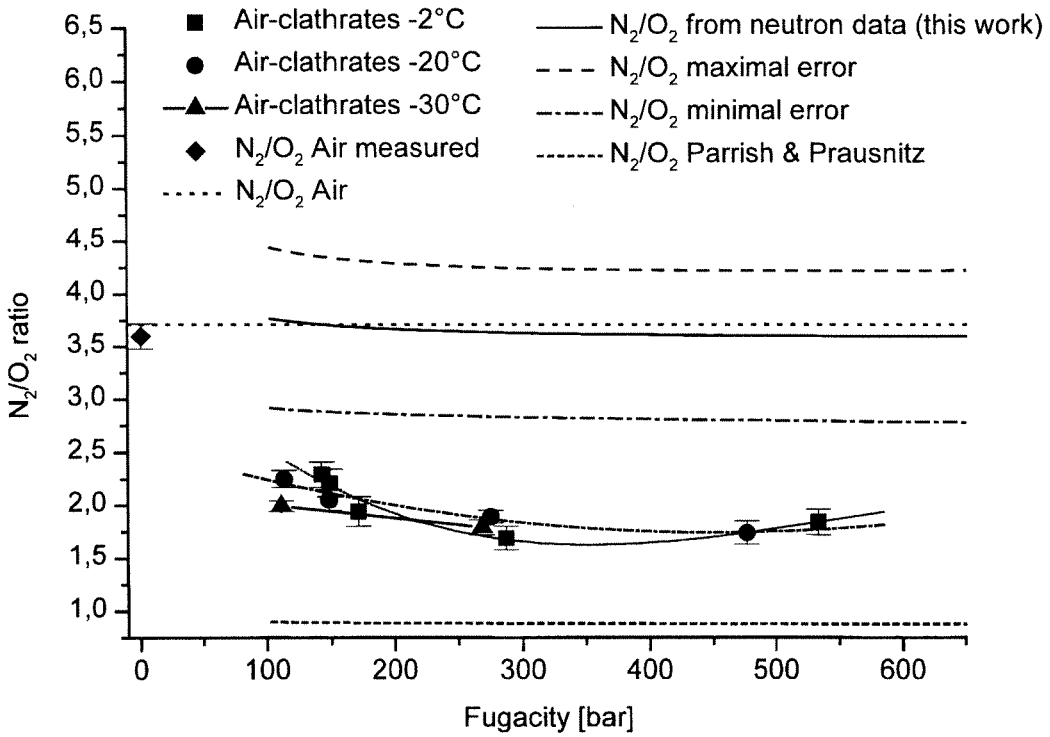

Figure 2: The N_2/O_2 ratio measured by Raman-spectroscopy in synthetic air clathrates as a function of pressure. The fitted polynomial curves represent the N_2/O_2 ratio for the isotherms at –2°, –20 °C and –30 °C. The broken line at the bottom gives the N_2/O_2 ratio as calculated from the Langmuir constants according to Parrish and Prausnitz [18]. The full curve gives the N_2/O_2 ratio as calculated from the Langmuir constants obtained by fitting our neutron diffraction results for the cage filling; its upper and lower error limits are given as broken lines.

only the initial fractionation was established. The experimental results are shown in Fig. 2 and the resulting tentative phase diagram given in Fig. 3. The minimum observed N_2/O_2 ratio was 1.7 at pressures of 300 to 400 bar when formed at –2 °C, a situation which corresponds to a late nucleation in an overpressurized regime. A more relevant estimate of the possible fractionation effect at the lower end of the transition zone gives N_2/O_2 ratios in the vicinity of 2.0 for the GRIP ice core. No detailed information is available on the fractionation at lower temperatures corresponding to the conditions found in the VOSTOK ice core. However, as indicated in Fig. 2, one may expect higher oxygen enrichment at lower temperature which is partly offset by the lower pressure

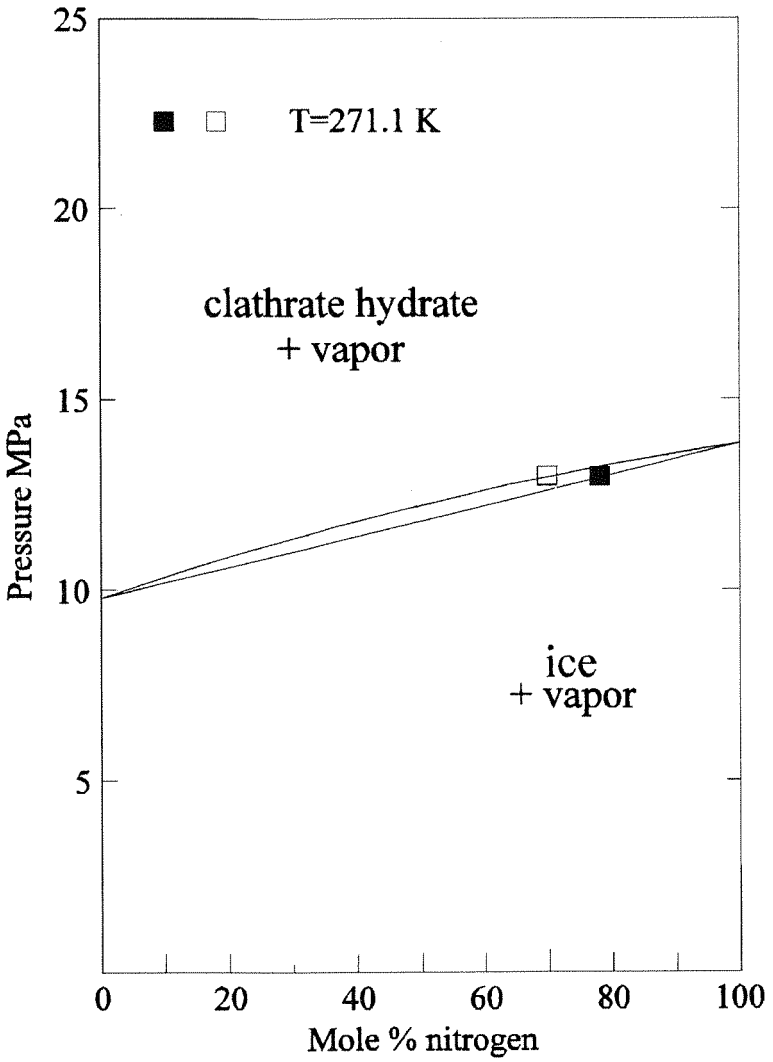

Figure 3: The tentative phase diagram for the N_2-O_2-H_2O system at –2 °C. The formation and decomposition points have been established only for one composition; the corresponding curves are given as a guide to the eye only.

at the end of the transition zone at VOSTOK. A linear extrapolation of the temperature effect results in a N_2/O_2 ratio of 1.9 to 2.0 for the lower end of the transition zone at VOSTOK. Thus the thermodynamic enrichment of oxygen from air in ice cores is seemingly limited to a N_2/O_2 ratio close to 2; the concomitant nitrogen enrichment in the remaining surrounding air could certainly result in a N_2/O_2 ratio as large as 6 or 7 (see Fig. 3). It should be noted at this stage that kinetic processes might take place in addition to thermodynamic ones which are able to produce even bigger fractionation effects; these will be discussed in section 3.3.

Little is known about possible fractionation effects involving the trace gases CO_2 and CH_4. The pure systems of these gases have been investigated repeatedly, however the focus was usually on measurements above the melting point of ice Ih. Some data at lower temperature are available for CO_2; for a review see Ref. 6. The fractionation effect in the N_2-CH_4 system was analysed for the solid clathrate phase in the vicinity of and above 0 °C [19] (Fig. 4). It seems likely that CH_4 is co-clathrated with air and should therefore be found in the air-hydrate crystals. Unfortunately, a direct proof by Raman spectroscopy is not possible due to the limited sensitivity of the method.

It should also be mentioned that a theoretical calculation of the various fractionation effects by a statistical thermodynamic approach was first proposed by Parrish & Prausnitz [18]; as an example of some relevance their results for the N_2-CH_4 system are also shown in Fig. 4. As may be seen from these results, the success of such calculations is still somewhat limited. This is likely to be due to some unjustified assumptions of the underlying theory. For example, there is no solid experimental proof that the filling behaviour of the gas components really follows a Langmuir isotherm (see section 2.3 below). This filling in turn enters into the calculation of the chemical potential of water in the mixed hydrate, which itself determines the stability lines.

For pure CH_4 clathrate, the decomposition temperature at 100 kPa (i.e. atmospheric pressure) is approximately 193K. It should be noted here that CH_4 is known to be physi-sorbed on ice surfaces below the decomposition pressure, at least at low temperatures; the coverage of the surface depends, of course, on the gas pressure but also seems to depend on the number of defects at the surface [20]. No information exists as to the preferential adsorption for CH_4 in air below the clathrate formation pressure threshold. Similarly for CO_2 in air, no detailed physico-chemical work is known for (preferential) physisorption on ice surfaces. Only the clathrate decomposition line was established and summarized by Davidson et al. [21]. The decomposition line cuts the value of 100 kPa (i.e. atmospheric pressure) at approximately 218 K. Below approximately 120 K, and in contrast to the CH_4-case, CO_2 clathrate seems to be unstable against solid CO_2 and ice Ih [21]. There is accumulated evidence for a preclathrate cage-like water arrangement around dissolved gas molecules in liquid water [22] or in the gas phase [23]. It may be suspected that similar local arrangements are also found at the surface of ice, at least near the melting point.

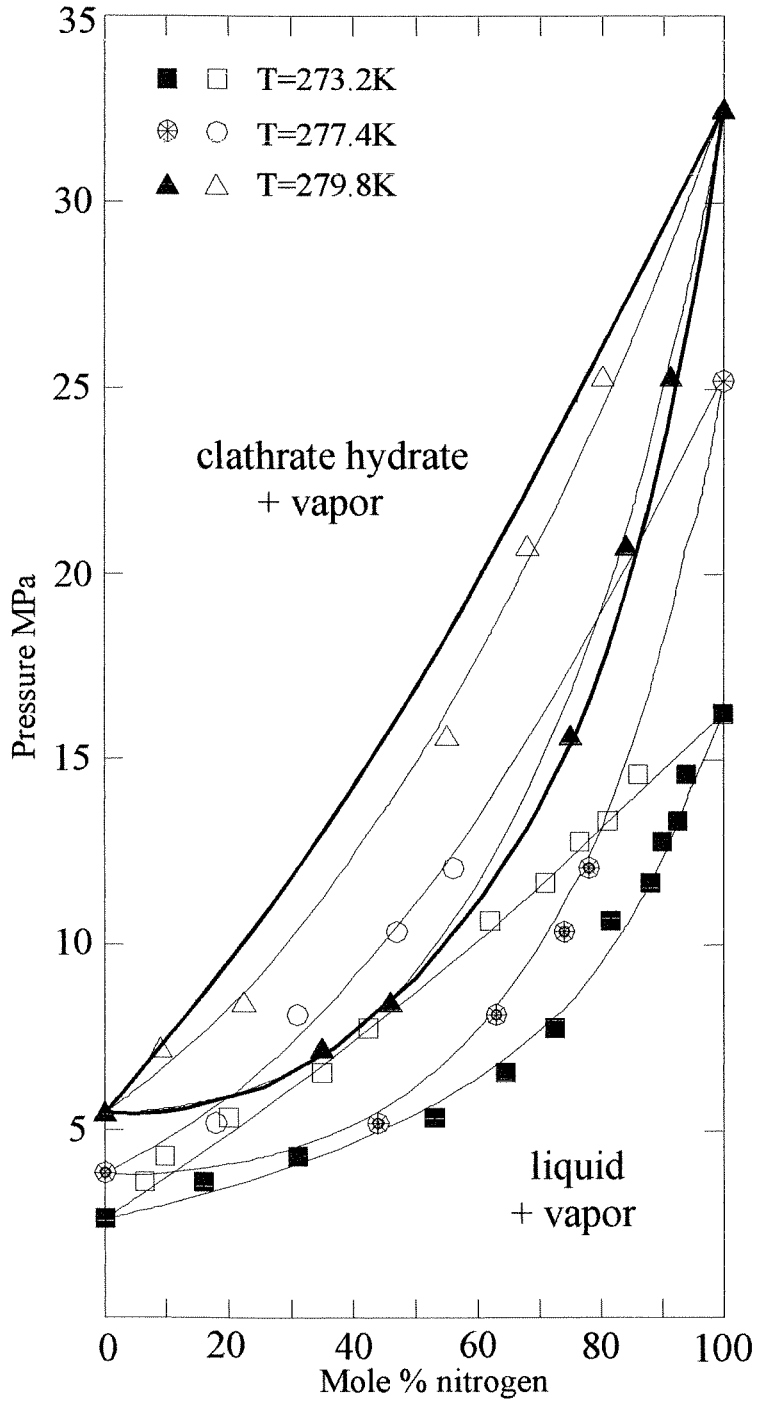

Figure 4: The phase diagram for N_2-CH_4-H_2O. The thin lines are given as a guide to the eye. The thick lines give the calculated equilibrium for a temperature of 279.8 K according to Ref. 18. Note that there is a change from a type I structure for pure CH_4 hydrate to a type II structure for pure N_2 hydrate, the exact location of which is not known.

2.3 Crystallography and stoichiometry

In situ neutron diffraction work [24, 25] over the last few years has allowed us to establish the cage filling for both small and large cages as well as the lattice constants as a function of pressure and temperature. From these data the density, thermal expansivity and compressibility of (deuterated) clathrate hydrates can be determined. The gas filling usually increases with increasing fugacity (pressure) of the gas; however, it does not necessarily, as previously assumed [e.g. 9], follow a Langmuir isotherm. Figures 5, 6 and 7 show the filling as a function of fugacity (pressure) for the small and large cages of N_2 and CO_2. The situation for air clathrate is not known in great detail but may be expected to be similar to the N_2 clathrate case.

The clathrate mass density will increase in a nonlinear way with the increasing overburden pressure as a function of both increasing fugacity as well as increasing mechanical pressure. It is important to note that the isosteric density (as obtained by applying mechanical pressure to the material at constant filling) is different from the equilibrium density obtained when clathrate crystals adjust their filling by re-growing at a given gas pressure. Isosteric and equilibrium unit cell volumes

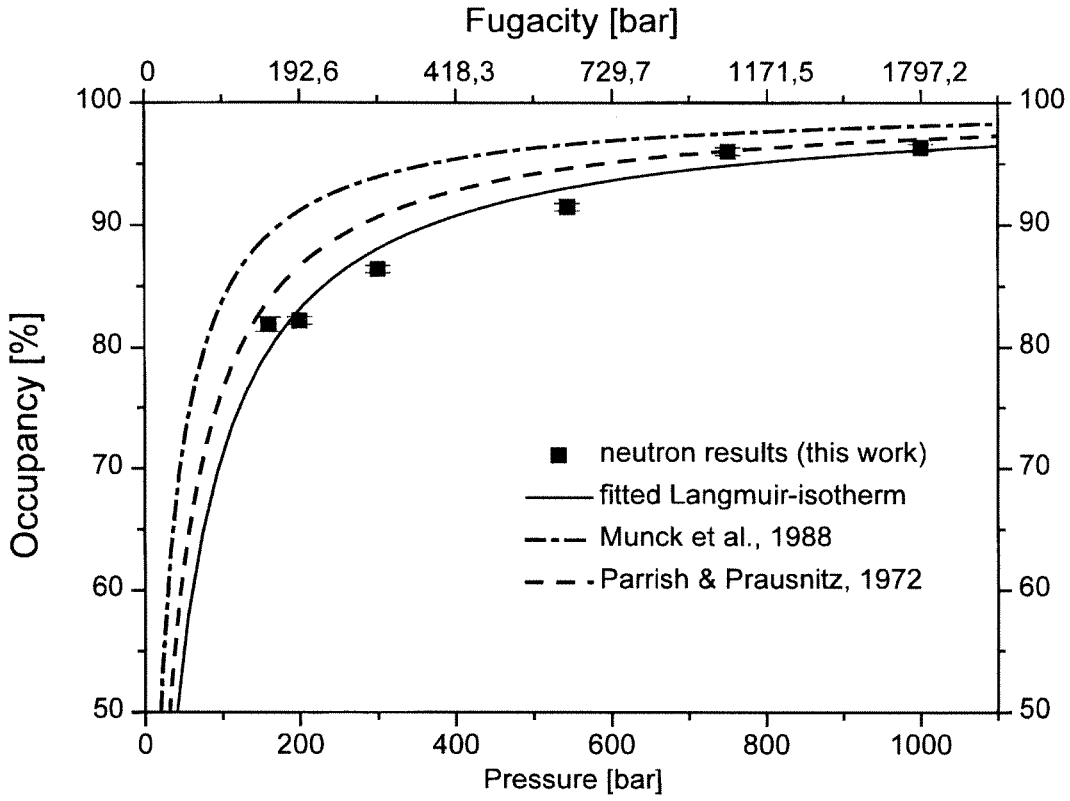

Figure 5: Filling of the small cages of N_2 clathrate vs. fugacity and pressure. The Langmuir isotherm fitted to the data as well as predicted isotherms taken from literature are shown (Ref. 15 and 26). The fitted Langmuir constant is $C_{SC} = 24.9(1.9)\ kbar^{-1}$.

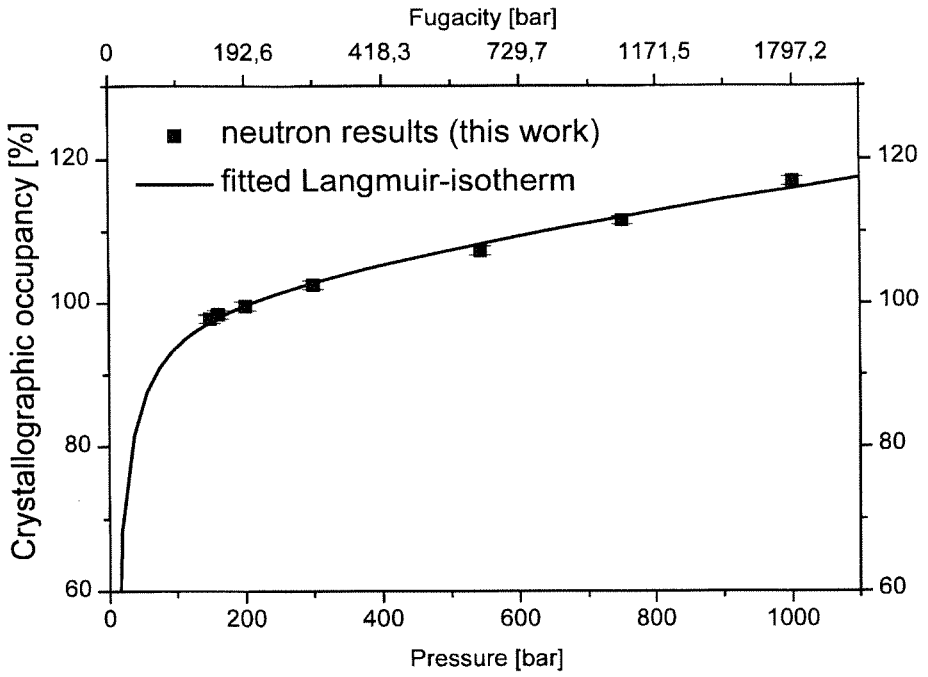

Figure 6: Filling of the large cages of N_2 clathrate vs. fugacity and pressure together with a fitted isotherm using a two constant model [24] with $C_{LC,single} = 205(44)\ kbar^{-1}$ and $C_{LC,double} = 0.125(6)\ kbar^{-1}$.

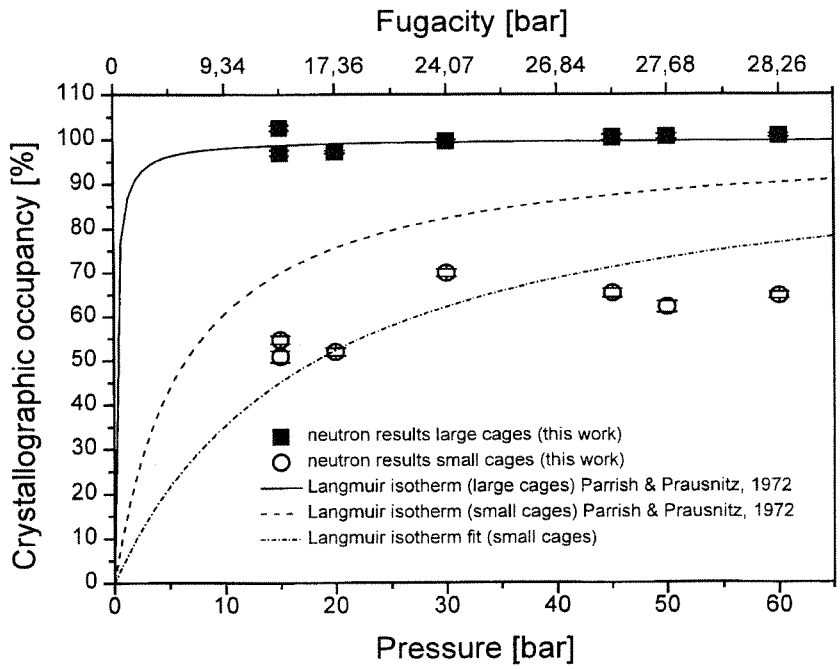

Figure 7: Filling of the small and large cages of CO_2 clathrate vs. fugacity and pressure. Clearly the fitted Langmuir constant is not a good representation of the data.

are given as a function of pressure in Fig. 8. Considering the geological timescales of the pressure increase in ice sheets one can safely assume that the filling behaviour is following the isothermal, and not the isosteric, pattern. However, there is good evidence that this is not true in laboratory experiments for timescales of hours and days.

Information on the expansivity and compressibility may be obtained from the temperature and pressure derivative of the unit cell volume as obtained by neutron powder diffraction. The thermal expansivity of air or N_2 clathrate hydrate was not measured in detail; however, it can be assumed that it is somewhat larger than for ice Ih and similar to other clathrate hydrates [27, 28]. It should again be noted that there is a difference between isosteric and isobaric thermal expansivity. At low temperatures the measurement of true isobaric thermal expansivities need constant readjustment of the cage filling which may take very long times and in fact may never be achieved even on geological timescales. The compressibility of type II N_2-clathrate hydrate was found to be distinctly smaller than of ice at the same temperature [24]. The isothermal compressibilities of N_2 and air clathrate hydrate are very similar.

2.4 Other properties

The elastic constants of air hydrate, or any other type II clathrate hydrate, are not known in any detail. Whalley [29] has given arguments to suggest that the elastic properties for ice Ih, a type I and a type II clathrate hydrate are not very different. Reliable information on compressibilities were obtained from diffraction experiments (section 2.3 above).

The static permittivity of clathrate hydrates is generally smaller than that for ice Ih. For example, N_2 clathrate hydrate has a static permittivity of 61 at –40 °C whereas

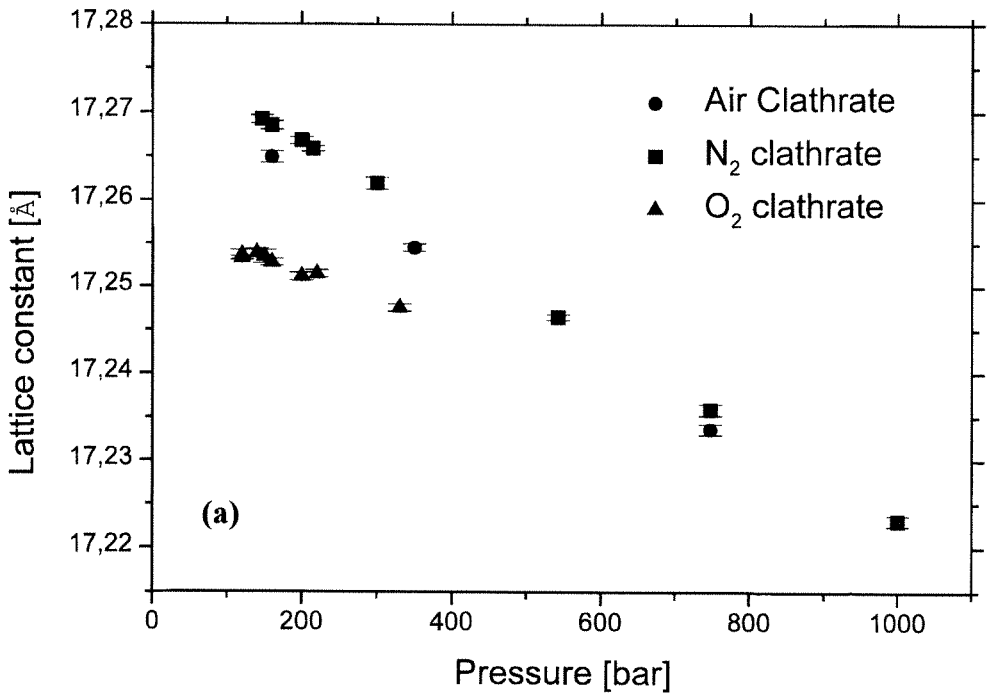

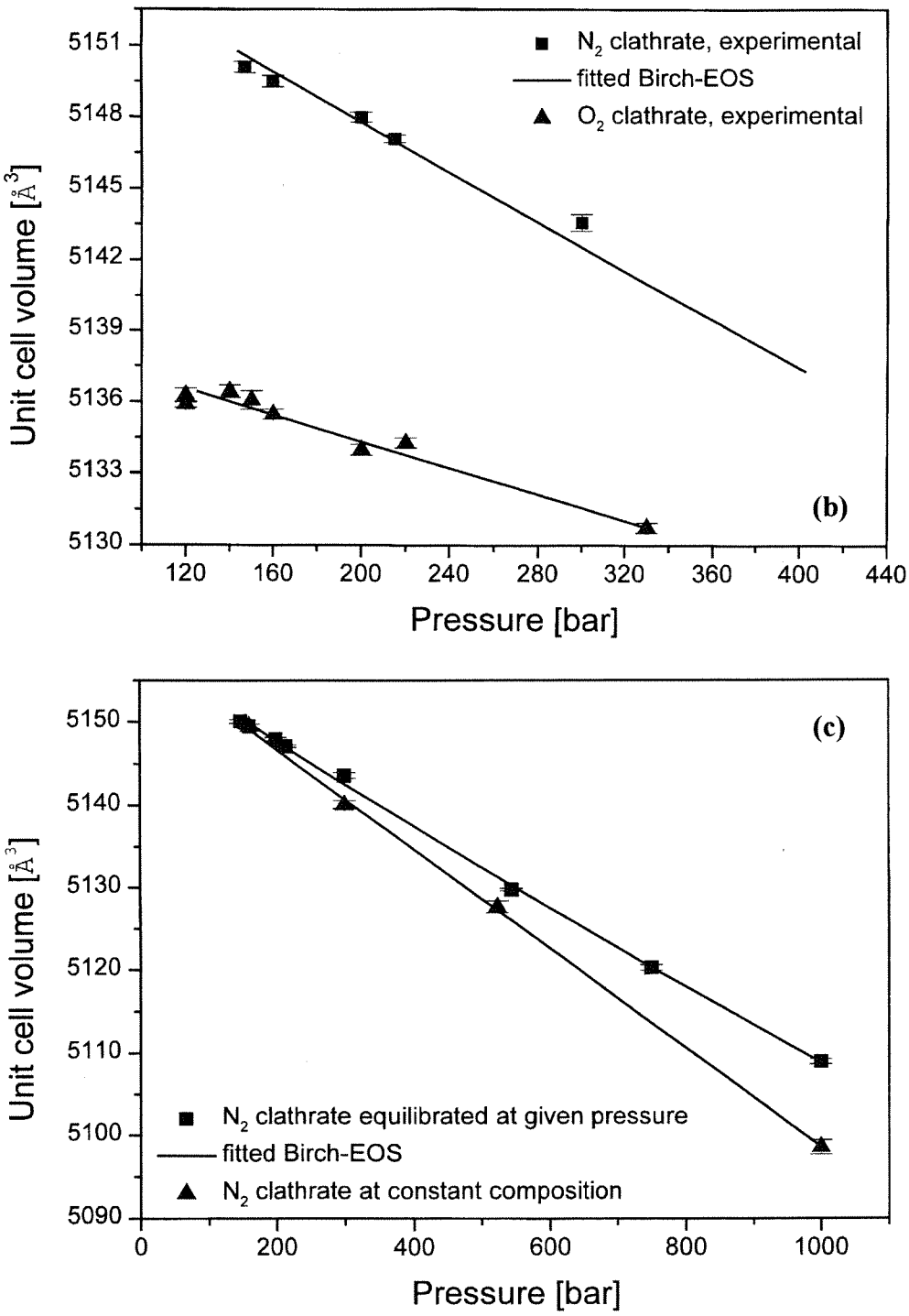

Figure 8: Lattice constants and unit cell volume of N_2, O_2 and air clathrate hydrates vs. pressure. (a) Cubic lattice constants vs. pressure. (b) Unit cell volume and fitted Birch equation-of-state at low pressure. (c) isosteric and isothermal unit cell volumes and fitted equation-of-states. For a discussion see text.

ice Ih has a static permittivity of 105 at the same temperature [30]. Likewise the high-frequency permittivity is 2.81 as compared to 3.2 for ice Ih. The relaxation time for water molecule reorientation, obtained from the maximum dielectric loss, is 180 μsec for N_2 clathrate as compared to approximately 1msec for ice Ih, again at –40 °C. The corresponding activation energies of the water molecule reorientation is 7.9 and 13.2 kcal·mol^{-1} for N_2-clathrate (at 120 MPa) and Ice Ih respectively [30]. This suggests that the local reorientation of water molecules in clathrates is somewhat faster than in ice Ih, yet the clathrate as a whole is less polarisable than ice Ih.

The refractive index of air clathrate was measured on a natural sample from the VOSTOK core using a Mach-Zehnder interferometer as 1.3137(16) at 270.2 K [31]. This is slightly larger than the (isotropically averaged) value of ice Ih at similar conditions. The difference is sufficient to clearly identify, visually, air hydrate inclusions in ice core samples under the optical microscope.

3. Non-equilibrium properties

3.1 Thermal conductivity

The thermal conductivity of clathrate hydrates is known to show an anomalous temperature dependence [32, 33], in that one observes a decrease with decreasing temperature. The experimental data show no strong dependence on neither the structure type (I or II) nor the guest species. The conductivities of air clathrates were not measured; however, one may safely assume similar values to those measured for THF clathrate (0.49 and 0.50 Wm^{-1}K^{-1} at 200 and 250 K respectively). This is several times less than that for ice Ih, which can be understood in terms of a simple Debye mean free path model [33].

3.2 Mobility and diffusion

The transport properties of the main constituents and defects of ice Ih have been dealt with in a large number of investigations. Considerably less is known about these properties in clathrate hydrates and very little information is available for air or N_2 hydrate. It seems likely that the volume self-diffusion of water molecules in air hydrates occurs via an interstitial mechanism as in ice Ih, with the additional complication however that the process will depend on the pressure- (fugacity-) dependent cage filling; little is actually known about the exact value of the diffusion constant and the activation energy. For ice Ih the corresponding numbers are D_{wi} (self-diffusion constant in ice Ih) $\approx 5.6 \cdot 10^{-15}$ m^2 s^{-1} and E_{wh} (activation energy for self-diffusion) ≈ 0.56 eV at the melting point [34, 35] ($D_{wi} \approx 2.4 \cdot 10^{-15}$ m^{2}s^{-1} at 263 K [36]). The diffusion constants of N_2 and O_2 in air hydrates and ice Ih are not known from direct measurements and are too small to be easily measured in a laboratory experiment. However, the latter may be estimated from observations of the crystal growth in ice cores from deep ice sheets. Some constraints on the relative diffusion constants of air molecules and water molecule diffusion in air hydrates were established by modelling the clathrate growth from air bubbles in ice sheets [37] (section 4.2 below). There are a number of indications that the grain boundary diffusion of water molecules is several orders of magnitude faster than in the bulk [e.g. 38]. Likewise, it can be expected that the surface diffusion of water molecules for ice Ih is at least at this level.

3.3 Plastic deformation

The mechanical strength of type II gas hydrates is not known; however, it is likely to be similar to type I gas hydrates, for which some information is available [39, 40]. In contrast to polycrystalline ice Ih which exhibits sharp yielding, subsequent strain softening and steady-state flow, the creep curves of CH_4-clathrate hydrate show monotonic strain hardening up to over 15 % of strain with a smaller temperature dependency than ice Ih. The measured [39, 40] yield strength is 85 MPa at 200 K with a strain rate of $3.5\times10^{-4}s^{-1}$. Thus clathrate hydrates are likely to behave as rather rigid units when embedded in an ice matrix subjected to viscoplastic deformation processes.

4. Growth and decomposition

4.1 Nucleation

It is generally accepted that nucleation of clathrate hydrate crystallites is a difficult process and, at least concerning the nucleation at an ice Ih surface, is not a well studied matter. Considerably more effort has been devoted to the technologically more important nucleation of natural gas hydrates from the liquid phase [6]. Nucleation at an ice surface requires gas molecules to slow down and attach themselves to the surface, as well as the subsequent enclosure of the gas molecules by surface diffusion or by a sublimation-condensation cycle of water molecules. Several of those embryonal gas-water cages of different size have to join together in order to form a nucleus of a type I or type II clathrate structure; this process is shown schematically in Fig. 9.

A belief, widely held in physical chemistry, is that nucleation in some systems is a stochiastic process [e.g.41, 42] and, correspondingly, a mathematical similarity with the process of radioactive decay exists. If this holds true then the time lag between reaching the thermodynamic conditions for stability and the actual onset of nucleation, referred to as the "induction time", is unpredictable for a given sample. In this case, the number of nucleated samples, from a total of N_0 samples, is given by:

$$N(t) = N_0 \cdot \exp(-\lambda t)$$

where λ is the nucleation rate. The mean induction time τ $(=1/\lambda)$ will depend on several factors, like the amount of supercooling or overpressure, the activation energy of diffusion of the constituents or the impurity content at the nucleation interface. There is some evidence that the nucleation of air clathrate hydrates in ice cores may follow such a scheme. The coexistence region of air bubbles and clathrate crystals extends in general to several hundred meters of ice in the so-called transition zone. This zone is equivalent to a time span of approximately 30 kyrs in the VOSTOK core and approximately an order of magnitude shorter for the GRIP core. Such a difference in time scale may appear surprising at first but could well be due to the temperature difference. Lower temperatures, as experienced at VOSTOK, will affect dramatically the surface mobility of water molecules, thus hampering considerably the basic gas enclathration step of the nucleation. Nucleation studies on natural samples by pressurization in the laboratory gave upper limits on the excess pressure needed [43, 44]. As the time scales of these experiments are several orders of magnitude shorter, in terms of the rate of pressure increase, care must be

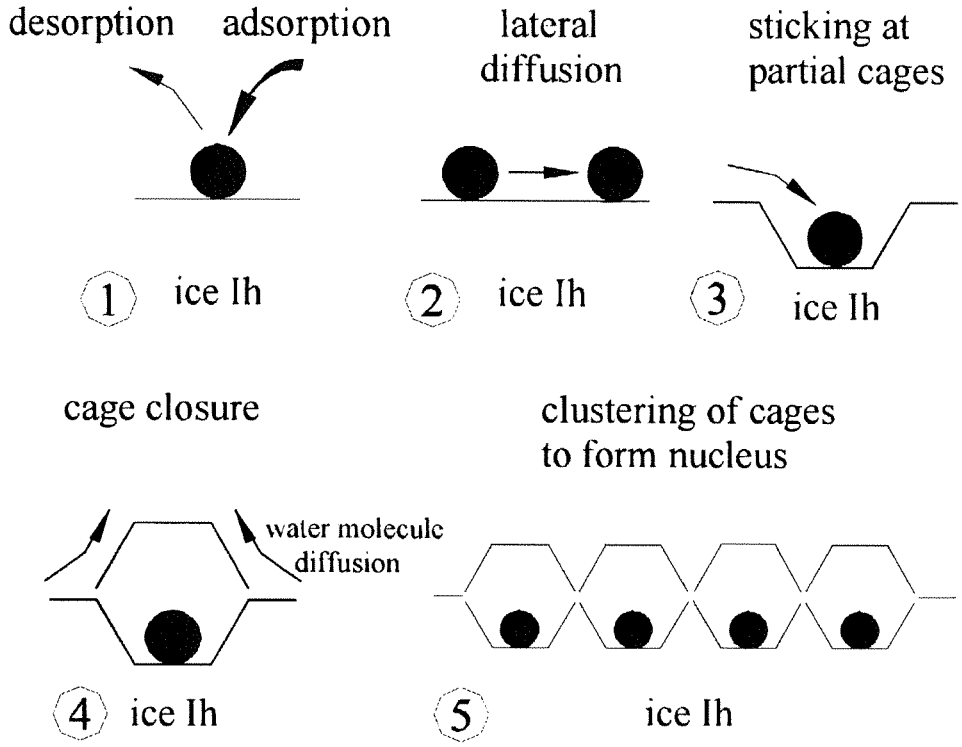

Figure 9: Basic steps for the nucleation of a clathrate hydrate crystallite on the surface of ice Ih. The figure is rather schematic as no details of the molecular mechanisms, the involved energies or rates are known.

taken when transferring these results to the actual process in ice sheets.

While it is certainly true that many air hydrate inclusions in ice cores are monocrystalline, there is recent evidence [45] from the top of the transition zone of the NGRIP core that some inclusions initially form as a polycrystalline aggregate. This seems to be somehow in contradiction to the stochiastic nature of the rather difficult nucleation process, but may find an explanation in a local, structurally faulty ice matrix or high, local impurity contents, thus rendering a (multi-)nucleation process much more likely. In fact, at highly faulty ice-bubble interfaces multinucleation will probably occur as soon as the stability field for clathrate hydrates is reached. The resulting polycrystalline aggregates may mechanically separate at later stages by plastic deformation processes of the ice in a mechanism similar to boudinage (see also section 3.3 above).

4.2 Growth

The growth of air clathrate hydrates from air bubbles and the later hydrate re-growth has been studied in a number of papers through laboratory experiments and theoretically[46, 47, 48, 49, 50]. A

schematic representation of the initial growth process is shown in Fig. 10.

It is now generally accepted that, after a sometimes rather long induction time (see section 4.1 above), the growth process itself is rather fast and mainly limited by the plastic deformation of the surrounding ice matrix; this process is necessary to maintain the dropping bubble pressure at the growing interface at least at the decomposition pressure. A detailed growth model was developed on the basis of rheological and diffusive properties of the ice-air hydrate system [37]. There is some evidence from laboratory experiments on natural samples that the growth in a bubble takes place mainly at the interface of gas and hydrate (and not at the hydrate-ice interface). Thus it seems that the diffusive transport of water molecules through the clathrate is more effective than the transport of air to the hydrate-ice interface. Nevertheless, the diffusion coefficient of water in air-hydrate was estimated to be one order of magnitude smaller than the one in ice [37]. The latest estimates of the air diffusion coefficient in ice are in the order of 10^{-21} m^2s^{-1} with O_2 diffusion approximately 2-3 times larger than that for N_2 [15]. Likewise from experimental observations on hydrate growth and model constraints, it was deduced that the diffusion coefficients of gas molecules in air hydrate crystals are, at least, two orders of magnitude smaller than those in ice [37].

Even after completion of growth and consumption of all free gas in a bubble there are, it seems, further re-growth processes taking place which exchange constituents within and between different neighbouring air clathrate crystals as well as neighbouring gas bubbles. These processes lead on one hand to some homogenization of the distribution of air constituents in a zoned crystal [14, 51], and on the other hand possibly to some kinetic fractionation due to the different diffusion coefficients of N_2 and O_2 in ice [15]. Oxygen seems to be enriched in the hydrate leaving nitrogen enriched air bubbles. In addition, due to the Gibbs-Thomson concentration difference in the vicinity of air hydrate crystals of different size [47], there seems to be a preferential growth of larger crystals on the expense of smaller ones. Microscopic observations have revealed that the presence of air hydrate crystals hinders the grain boundary migration of ice crystals thus influencing ice recrystallization [52]. From such crystals at grain boundaries, the surface energy of air hydrate crystals can be estimated and is of a similar magnitude as that for ice Ih [53]. Attempts have been made to correlate the number occurence and size distributions of hydrate crystals to the climatic conditions in which the surrounding ice matrix was formed [50]. Clearly this undertaking is not an easy one. In order to reveal details of the initial conditions, one has to understand all steps of the (trans)formation processes. While there is good evidence that the number concentration is higher during cold climate stages, other points remain unresolved. Open questions, for example, concern the amount of air dissolved in slip bands or at grain boundaries (which may explain the discrepancies between the measured amount of air and the estimate from the number and size of the clathrate crystals [50]) or the influence of various impurities on the transport properties of the constituents.

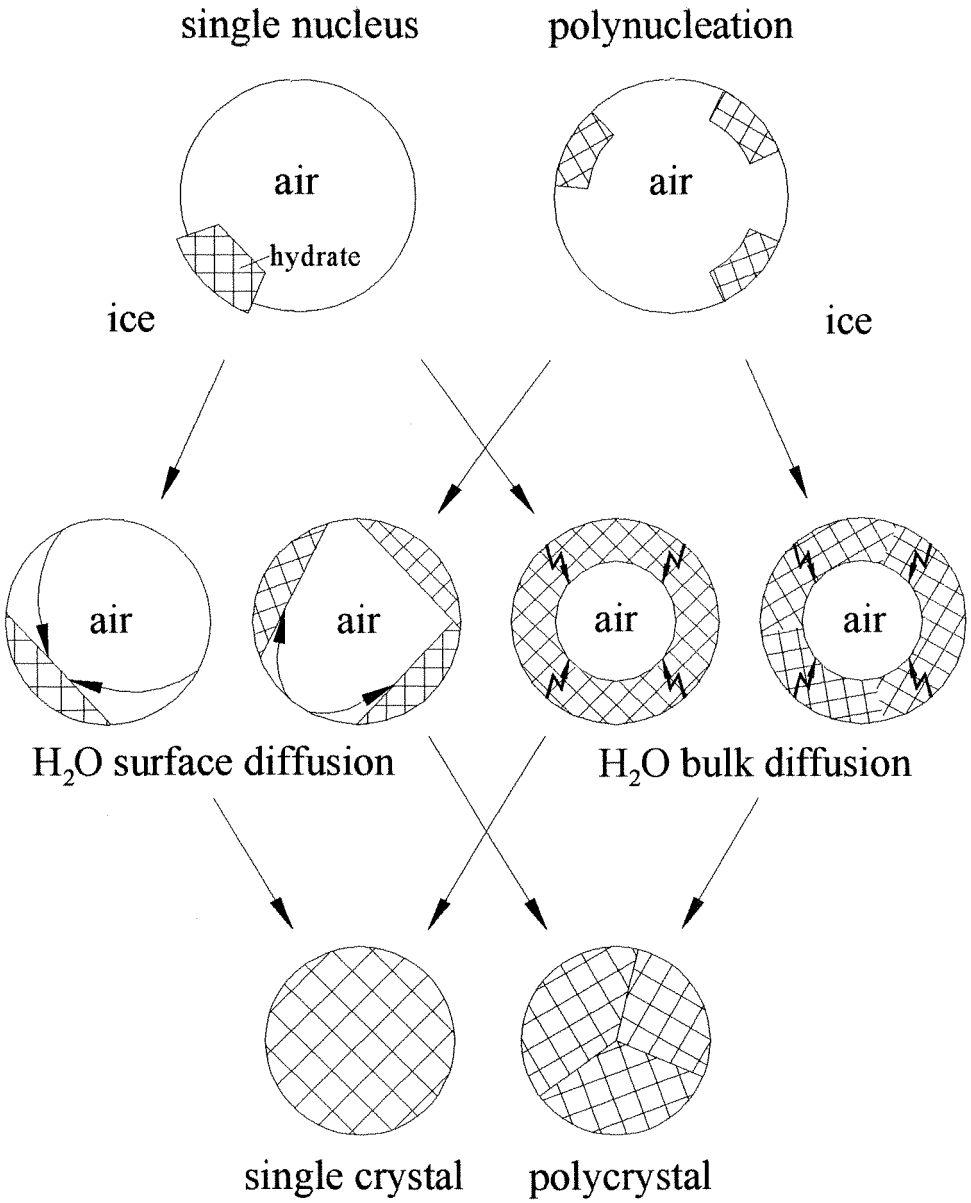

Figure 10: Schematic picture of the clathrate growth from an air bubble. The growth starts either with a single nucleus or nucleation occurs at several places at the bubble-ice interface. Concentric growth (r.h.s. of the diagram) is often observed in laboratory experiments possibly linked somehow to multinucleation. Linear growth (l.h.s. of the diagram) should be prefered when a single nucleus is formed. The growth could take place either into the space of the air bubble or into the surrounding ice matrix. It is not known with certainty which of the directions dominate in the natural environment, however the mechanical relaxation of the surrounding ice will in all cases lead eventually to an approximately spherical clathrate hydrate aggregate.

4.3 Decomposition

After core recovery, slow relaxation processes take place in the ice matrix eventually leading to a loss of confining pressure and a subsequent decomposition of air hydrate crystals into "secondary" air bubbles. Storage at low temperatures slows down the process considerably and temperatures < –50 °C are advisable [54] for storage of clathrate containing samples over many years. On the other hand, decomposition within a few minutes is desired when analysing the gas content of the cores. Milling techniques are used to analyse the CO_2 content and it seems that problems with retarded release of CO_2 gas is connected somehow to clathrate metastability below the decomposition pressures [e.g. 55]. The low temperature inhibition mechanism of clathrate decomposition is not known in any detail. The existence of metastable gas hydrates has also been observed in permafrost regions and was confirmed in laboratory experiments [56]. One may speculate that two processes play a role: (1) decomposition, via gas release from the surface, may be retarded, on a molecular level, for clathrate crystals covered in molecularily bound ice as the bulk diffusion of gas through ice Ih is very slow, and (2) local formation of individual clathrate cages (most likely pentagondodecahedra) at the ice surface may bind gas in a physi-sorbed state. In the latter process different gases could well behave differently; however, possible fractionation effects of the air constituents due to preferential adsorption at the ice surface are presently not understood in detail.

5. Conclusion

This review certainly demonstrates that in several respects a deeper understanding of the chemico-physical behaviour of air in contact with ice is not yet obtained. It is well established that the presence of air modifies the habitus of growing snow crystals [57] at pressures far removed from the stability field of air clathrates. Thus the interaction of air with the surface of ice is clearly noticable even at low fugacities. The interaction between air and ice takes place initially in the falling snow, later in the snow and firn layer, and finally during core recovery [58], and needs to be understood when attempts are made to reconstruct the details of the paleoatmosphere and the paleoclimate from ice core records. At higher fugacities, relevant to most of the questions discussed here, the situation becomes even more complex. In most cases it is still an open question how this interaction takes place on a molecular level at the surface and in the bulk of ice. More data from deep ice cores will be helpful to gain further insight into the processes taking place on geological time scales. The most challenging task however is to connect these field observations with laboratory experiments as well as computer simulations on a molecular level. To build this bridge it will be important to establish and verify macroscopic and mesoscopic models based on information of interactions at a molecular level. First steps in this direction have been made by several groups and others are to follow.

Acknowledgement

The authors thank Drs S. Kipfstuhl, F. Pauer, A. N. Salamatin and H. Shoji for helpful discussions and the Institut Laue-Langevin/Grenoble for granting beam time and financial support. Part of the work was supported by the Deutsche Forschungsgemeinschaft (grants Ku920/3 and Ku920/4) and the European Commission (contract N° ENV4-CT96-5048).

References

1. S.L. Miller, *Science*, 165, 489 (1969).
2. A.J. Gow, H.T. Veda, and D.E. Garfield, *Science*, 161, 1011 (1968).
3. A.J. Gow, *J. Geophys. Res.*, 80, 5101 (1971).
4. A.J. Gow, and T. Williamson, *J. Geophys. Res.* 80, 5101 (1975).
5. H. Shoji and C.C. Langway, *Nature*, 298, 548 (1982).
6. E.D. Sloan, *Clathrate Hydrates of Natural Gases*, Marcel Dekker, New York, 1998.
7. M. von Stackelberg and H.R. Müller, *Z. Elektrochem.*, 58, 25 (1954).
8. T. Hondoh, H. Anzai, A. Goto, S. Mae, A. Higashi, and C.C. Langway, *J. Incl. Phenom.*, 8, 17 (1990).
9. J.H. van der Waals and J.C. Platteeuw, *Adv. Chem. Phys.*, 2, 1 (1959).
10. H. Shoji, and C.C. Langway, Jr., *J. Physique C1*, 551 (1987).
11. A. van Cleef, and G.A.M. Diepen, *Rec. Trav. Chim.* 79, 582 (1960) and 84, 1085 (1965).
12. J. Nakahara, Y. Shigesato, A. Higashi, T. Hondoh, and C.C. Langway, Jr., *Phil. Mag. B*, 57, 421 (1988)
13. F. Pauer, J. Kipfstuhl, and W.F. Kuhs, *Geophys. Res. Lett.*, 22, 969 (1995).
14. F. Pauer, J. Kipfstuhl, and W.F. Kuhs, *Geophys. Res. Lett.*, 23, 177 (1996).
15. T. Ikeda, H. Fukazawa, S. Mae, L. Pepin, P. Duval, B. Champagnon, V.Ya. Lipenkov, and T. Hondoh, *Geophys. Res. Lett.* 26, 91 (1999).
16. T. Ikeda, H. Fukazawa, S. Mae, T. Hondoh, and C.C. Langway, Jr., *J. Phys. Chem. B*, 101, 6180 (1997).
17. B. Chazallon, G. Champagnon, G. Panzcer, F. Pauer, A. Klapproth, and W.F. Kuhs, *Eur. J. Mineral.*, 10, 1125 (1998).
18. W.R. Parrish and J.M. Prausnitz, *Ind. Eng. Chem. Process Des. Devel.*, 11, 26 (1972).
19. J. Jhaveri and D.B. Robinson, *Can. J. Chem. Engineer.*, 43, 75 (1965).
20. L. Chaix, J. Ocampo and F. Dominé, *C. R. Acad. Sci. Paris*, 322, 609 (1996).
21. D.W. Davidson, S.K. Garg, S.R. Gough, Y.P. Handa, C.I. Ratcliffe, J.S. Tse, and J.A. Ripmeester, *J. Inclus. Phenom.*, 2, 231 (1984).
22. D.T. Bowron, A. Filipponi, C. Lobban, and J.L. Finney, *Phys. Rev. Lett.*, 81, 4164 (1998).
23. Y. Yamamoto, T. Komai, and A. Wakisaka, *Rev. High Pressure Sci. Technol.*, 7, 1150 (1998).
24. W.F. Kuhs, B. Chazallon, P.G. Radaelli, and F. Pauer, *J. Inclus. Phenom.*, 29, 65 (1997).
25. W.F. Kuhs, B. Chazallon, A. Klapproth, and F. Pauer, *Rev. High Pressure Sci. Technol.*, 7, 1147 (1998).
26. J. Munck, S. Skjold-Jorgensen, and P. Rasmussen, *Chem. Eng. Sci.*, 43, 2661 (1988).
27. J.S. Tse, *J. Physique C1*, 48, 543 (1987).

28. J.S. Tse, W.R. McKinnon, and M. Marchi, *J. Phys. Chem.*, 91, 4188 (1987).
29. E. Whalley, *J. Geophys. Res.*, 85, 2539, (1980).
30. D.W. Davidson, *Clathrate Hydrates in Water: A Comprehensive Treatise*, Vol.2, pp.115-134 (1973).
31. T. Uchida, W. Shimada, T. Hondoh, S. Mae, and N.I. Barkov, *Appl. Optics*, 34, 5746 (1995).
32. R.G. Ross, and P. Anderson, *Can. J. Chem.*, 60, 881 (1982).
33. M.W.C. Dharma-wardana, *J. Phys. Chem.*, 87, 4185 (1983).
34. M. Oguro, T. Hondoh, and K. Azuma, in *Lattice Defects in Ice Crystals* (Ed. A. Higashi), Hokkaido University Press, Sapporo, 1988, pp.97-128.
35. T. Hondoh in *Physics and Chemistry of Ice* (Eds. N. Maeno and T. Hondoh), Hokkaido University Press, Sapporo, 1992, pp.481-487.
36. K. Satoh, T. Uchida, T. Hondoh, S. Mae, *Proc. NIPR Symp. Polar Meteorol. Glaciol.*, 10, 73 (1996).
37. A.N. Salamatin, T. Hondoh, T. Uchida, and V.Ya. Lipenkov, *J. Cryst. Growth*, 193, 197 (1998).
38. S.S. Johnsen, H.B. Clausen, J. Jouzel, J. Schwander, Á.E. Sveinbjörnsdóttir, and J. White in *Ice Physics and the Natural Environment* (Eds. J. S. Wettlaufer, J. G. Dash, and N. Untersteiner), NATO ASI Series, 56, Springer, Berlin Heidelberg 1999, pp. 89-107.
39. L.A. Stern, S. Kirby, and W.B. Durham, *Science*, 273, 1843-1848 (1996).
40. L.A. Stern, S. Kirby, and W.B. Durham, *Energy and Fuels*, 12, 201 (1998).
41. M. Baldwin, and B. Vonnegut, *Rev. Sci. Instrum.*, 53, 1911 (1982).
42. T.W. Barlow, and A.D.J. Haymet, *Rev. Sci. Instrum.*, 66, 2996 (1995).
43. T. Ikeda, T. Uchida, and S. Mae, *Proc. NIPR Symp. Polar Meteorol. Glaciol.*,7, 14 (1993).
44. T. Uchida, T. Hondoh, S. Mae, P. Duval, and V.Ya. Lipenkov, *Ann. Glaciol.*, 20, 143 (1994).
45. S. Kipfstuhl, F. Pauer, W.F. Kuhs, and H. Shoji, Submitted to Geophys. Res. Lett..
46. T. Uchida, T. Hondoh, S. Mae, P. Duval, and V.Ya. Lipenkov in *Physics and Chemistry of Ice* (Eds. N. Maeno and T. Hondoh), Hokkaido University Press, Sapporo, 1992, pp.121-125.
47. T. Uchida, S. Mae, T. Hondoh, V.Ya. Lipenkov, P. Duval, and J. Kawabata, *Proc. NIPR Symp. Polar Meteorol. Glaciol.*,8, 140 (1994).
48. T. Uchida, P. Duval, V.Ya. Lipenkov, T. Hondoh, S. Mae, and H. Shoji, *Mem. Natl. Inst. Polar Res., Spec. Issue*, 49, 298 (1994).
49. T. Uchida, T. Hondoh, S. Mae, V.Ya. Lipenkov, P. Duval, *J. Glaciol.*,40, 79 (1994).
50. F. Pauer, S. Kipfstuhl, W.F. Kuhs, and H. Shoji, *J. Glaciol.*, 45, 22 (1999).
51. F. Pauer, J. Kipfstuhl, and W.F. Kuhs, *J. Geophys. Res.*, 102, 26519 (1997).
52. T. Uchida, S. Mae, T. Hondoh, P. Duval, V.Ya. Lipenkov, *Proc. NIPR Symp. Polar Meteorol. Glaciol.*,7, 7 (1993).
53. T. Uchida, S. Mae, T. Hondoh, P. Duval, V.Ya. Lipenkov, *Proc. NIPR Symp. Polar Meteorol. Glaciol.*,7, 1 (1993).
54. T. Uchida, T. Hondoh, S. Mae, H. Shoji, and N. Azuma, *Mem. Natl. Inst. Polar Res., Spec. Issue*, 49, 306 (1994).

55. M. Anklin, J. Schwander, B. Stauffer, J. Tschumi, A. Fuchs, J.M. Barnola, and D. Raynaud, *J. Geophys. Res.*, 102, 26539 (1997).
56. E.D. Ershov, and V.S. Yakushev, *Cold Region Science Technol.*, 20, 147 (1992).
57. W. Beckmann, *J. Cryst. Growth*, 58, 443 (1982).
58. M. Bender, T. Sowers, and V.Ya. Lipenkov, *J. Geophys. Res.*, 100, 18651 (1995).